

Article

A New Method to Lightweight Magnesium Using Syntactic Composite Core

Penchal Reddy Matli ¹, Joshua Goh Yong Sheng ¹, Gururaj Parande ¹, Vyasraj Manakari ¹,
Beng Wah Chua ², Stephen Chee Khuen Wong ² and Manoj Gupta ^{1,*}

¹ Department of Mechanical Engineering, National University of Singapore, Singapore 117576, Singapore; mpeprm@nus.edu.sg (P.R.M.); e0177106@u.nus.edu (J.G.Y.S.); mpeguru@nus.edu.sg (G.P.); mbvyasaraj@u.nus.edu (V.M.)

² Singapore Institute of Manufacturing Technology, Singapore 138634, Singapore; bwchua@simtech.a-star.edu.sg (B.W.C.); ckwong@simtech.a-star.edu.sg (S.C.K.W.)

* Correspondence: mpegm@nus.edu.sg; Tel.: +65-65-166-358

Received: 10 June 2020; Accepted: 7 July 2020; Published: 11 July 2020



Abstract: Light weighting of magnesium-based materials is crucial for its extensive use in transportation applications. Hybrid processing of these materials in a shell-core pattern can substantially improve the specific properties of magnesium. In the present study, the Mg/Mg-20GMB (glass microballoon) hybrid composite was prepared using a disintegrated melt deposition technique. Microstructural characterization and mechanical properties of the developed as-cast Mg/Mg-20GMB hybrid composite were investigated. Results revealed that a unified metallurgical interface was formed between the Mg-20GMB core material and the pure Mg shell. Energy dispersive X-ray spectroscopy (EDX) results confirmed the existence of Mg₂Si as the secondary phase in the Mg-20GMB core material. The hybrid Mg/Mg-20GMB composite exhibited much superior compressive yield strength (↑71.6%), lower ultimate compressive strength (↓23.25%), and enhanced ductility (↑186.48%) when compared to as-cast pure magnesium.

Keywords: magnesium; syntactic foam; glass microballoons (GMB); hybrid composite; microstructure; compression; fractography

1. Introduction

The interest in lightweight materials in the aviation and car businesses has prompted broad, innovative work endeavors to further develop lightweight matrix composites using cost-effective fabrication techniques [1]. A reduction in weight would reduce the inertia of vehicles and aircraft, thereby reducing fuel consumption and subsequently decrease the amount of carbon dioxide (CO₂) produced [2,3]. To reduce CO₂ emissions and to improve fuel and energy efficiency, the automotive/aerospace industry has focused on reducing the overall weight of passenger vehicles/aircraft [4]. The weight of the vehicle body can be reduced by introducing lightweight materials. This research addresses the exploration of the relationship between the product and the production system when exploring novel materials. New automotive innovations are constantly being introduced to improve a vehicle's crash safety, drivability, and fuel economy, subsequently resulting in lower overall costs [4,5]. While cars in the past were made up of entirely steel-based products and subsequently of aluminum alloys, manufacturers are now transitioning towards magnesium and their composites that have the potential to deliver enhanced performance [4,5]. To accommodate these new materials, new manufacturing techniques must be introduced and optimized. In terms of manufacturing technique, disintegrated melt deposition is a viable option which uses a protective argon atmosphere instead of greenhouse gases like SF₆ and CO₂, which are expensive and also harmful

to the environment [1,6]. The feasibility of these new materials depends on several factors such as the added performance, raw material costs, and the manufacturing process, amongst others. In this context, the automotive industry is increasingly interested in smart material formulations, which enable lightweight construction.

Magnesium (Mg) is the lightest structural metal and is a popular material choice when it comes to weight-critical structural components, due to its low density and high strength to weight ratio [5,7]. This quality is especially useful for weight-critical uses in the aerospace, space, sports, and automotive industries [5]. The aerospace and automotive materials market is dominated by Al-based alloys and composites and merely replacing Al with suitable Mg materials can drastically reduce the fuel costs in transportation sectors, making it financially viable. Mg is about 33% lighter than Al, and both have similar strengths and melting points [8]. However, due to its hexagonal closed packed (HCP) structure, Mg is less ductile compared to Al, which has a face-centered cubic (FCC) structure [9–11]. While the ductility and strength of Mg can be increased by traditional alloying [12], the use of discontinuous reinforcement has improved many properties of Mg even beyond the limits of alloying [10,13–15]. Magnesium alloys have benefits of low density, high specific strength, and good castability, but the main drawbacks are low ductility and creep resistance [3,16]. With the ban on Mg-based materials lifted by the Federal Aviation Administration (FAA) in 2015, there is a renewed interest in developing high-performance magnesium materials for aerospace sectors [17]. In most cases, one single light metal material does not satisfy all the requirements of delivering high performance at a minimum cost [18,19]. Therefore, a significant concern in the manufacturing sector is the current production of advanced Mg-based hybrid composite materials, as they possess an excellent potential for commercial applications.

Hollow glass microballoons (GMB) are engineered hollow glass microspheres made of sodalime–borosilicate glass that is an alternative to typically used fillers such as cenospheres [20,21]. GMB particles are excellent additive materials that are used in various industries like automotive, aerospace, heavy truck, electronics, electrical, appliance, durable goods industries, and construction products due to their low-density for many purposes such as weight reduction, reduction in thermal expansion, abrasion resistance improvement, as well as to save process and material costs [22,23]. The current research is aimed at exploring the possibility of using GMB particles for the development of Mg-GMB syntactic foam as a core component through the combination of cold compaction and hot extrusion technique. Therefore, the manufacturing of Mg-based hybrid composite materials is likely to be a promising solution for future industrial needs. Compound casting is a process of joining two metals or alloys through direct casting in which one component is in the liquid state (molten metal) and the other is in the solid-state form [24,25]. In this procedure, a solid component is mounted in the mold, and commercially pure metal or alloy melt is cast around it. Thus, a diffusion-reaction zone is formed at the interface of the melt and the solid insert that results in the bonding of the two metals/materials [26]. Producing complicated parts by utilizing this procedure is simple and less tedious.

This study aims to propose a novel process to produce pure Mg and Mg/Mg-20 wt.% GMB hybrid composite by the disintegrated melt deposition (DMD) technique, and to investigate the effect of the interfacial microstructure on the mechanical response of the as-cast hybrid composite.

2. Materials and Methods

2.1. Materials

In this work, magnesium turnings with 99.9% purity (ACROS Organics, Morris Plains, NJ, USA) were used as the base material. Hollow glass microballoon (GMB) particles with a diameter of 11 μm having a density of ~ 1.05 g/cc were acquired from Sigma Aldrich, Singapore. The compositions of materials used in the present study are: (i) pure Mg and (ii) Mg/Mg-20GMB hybrid composite. Powder metallurgy with hot extrusion followed by disintegrated melt deposition techniques were used to produce the Mg/Mg-20GMB hybrid composite.

2.2. Specimen Preparation

2.2.1. Blending, Compaction, and Hot Extrusion

In the first step, to produce the Mg-20GMB core material, 20 wt.% of GMB powder and Mg turnings were weighed and blended at 200 rpm for 2 h using a high energy planetary ball mill (Retsch PM400) without the use of grinding balls, to avoid fracture of the hollow GMB particles. Then, the blended powder was compacted into cylindrical billets with 35 mm diameter and 40 mm length under a pressure of 97 bars (50 tons). Before hot extrusion, the compacted billets were homogenized at 250 °C for 1 h and extruded at 200 °C on a 150-ton hydraulic press producing rods of 20 mm in diameter. The schematic representation of the processing of Mg-20GMB core material is shown in Figure 1.

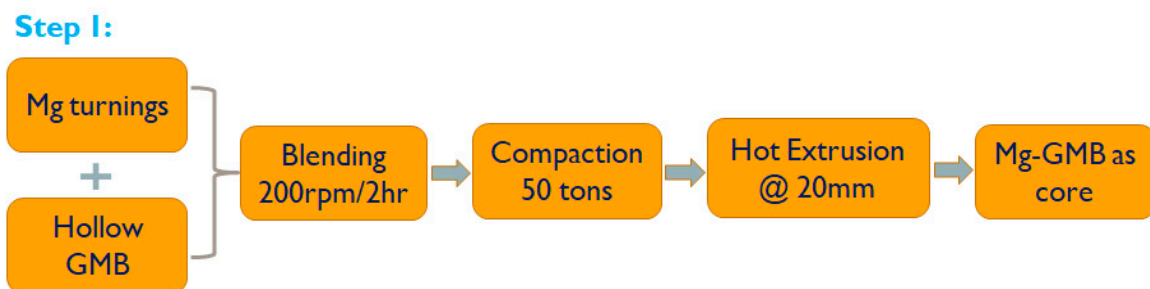


Figure 1. Schematic representation of the processing of core (Mg-20GMB) material.

2.2.2. Disintegrated Melt Deposition (DMD)

The disintegrated melt deposition (DMD) technique has successfully been used to synthesize various magnesium-based composites for almost two decades [1,12,20,27]. DMD has many advantages. It is energy efficient and produces 20–30% less material wastage compared to conventional casting methods. DMD is also able to provide composites with a homogeneous distribution of reinforcements and finer grain size. The product is a highly dense material with improved qualities [1]. Additionally, the use of argon gas in DMD is environmentally friendly and non-toxic to users.

In the second step, the Mg-20GMB extruded rod was used as core material, and Mg turnings were used as a base material. The extruded Mg-20GMB rod was placed at the center of the steel mold. Then, Mg turnings were superheated to 750 °C under an argon gas atmosphere. The superheated melt was stirred at 460 rpm for 5 min and bottom-poured. The melt was then released through a 10 mm diameter orifice at the base of the crucible. The melt was disintegrated by two jets of argon gas at a 25 litres per minute lpm flow rate. The disintegrated melt was directed at the core. Finally, a 40 mm diameter ingot was obtained. The schematic representation of the fabrication process is illustrated in Figure 2. For characterization, the samples were machined into a total diameter of 30 mm, where the outer shell of the hybrid composite was reduced to a thickness of 10 mm.

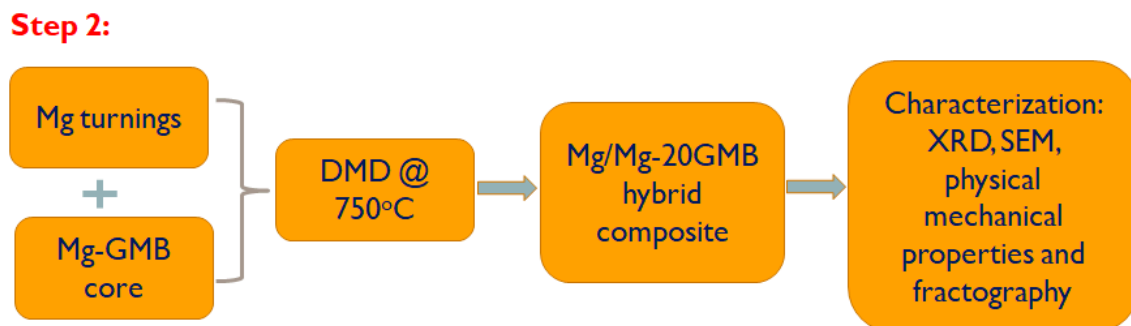


Figure 2. Schematic representation of the processing of Mg/Mg-20GMB hybrid composite.

2.3. Characterizations

Experimental and theoretical density measurements were performed on polished as-cast monolithic Mg and Mg/Mg-20GMB hybrid composite samples, using Archimedes' principle and the rule-of-mixtures principle, respectively. X-ray diffraction (XRD) analysis was carried out by using an automated Shimadzu LAB-XRD-6000 diffractometer (Kyoto, Japan). The specimens were subjected to Cu-K α radiation (0.1542 nm) with a scanning speed set at 2°/min. Grain size studies were performed on polished as-cast Mg/Mg-20GMB hybrid composite using a Leica DM 2500 M Optical microscope. Morphologies of the as-cast Mg/Mg-20GMB hybrid composite specimens were observed by the JEOL, JSM-6010 scanning electron microscope (SEM) equipped with a spectrometere to perform energy dispersive X-ray spectroscopy (EDX). The Vickers micro-hardness measurement of the cross-section of the as-cast hybrid composite was conducted on a Matsuzawa MXT50 automatic digital microhardness tester. Compressive tests were performed using a Shimadzu AG-25TB at room temperature on cylindrical as-cast pure Mg and Mg/Mg-20GMB hybrid composite. This test was carried out in accordance with the ASTM E9-89a standard method. The fracture surface of post-compression samples was analyzed using a JEOL, JSM-6010 scanning electron microscope (SEM).

3. Results and Discussion

3.1. Density Measurements and Porosity

Table 1 shows the results of the theoretical and experimental density and porosity of as-cast pure Mg, Mg-20GMB (core), and as-cast Mg/Mg-20GMB hybrid composite. It can be seen that the experimental densities of Mg-20GMB and Mg/Mg-20GMB hybrid composite are less than pure Mg due to the presence of lower density GMB (~1.05 g/cc) particles. It can be observed that porosity in the as-cast Mg/Mg-20GMB hybrid composite was found to be 1.73%. Mg-20GMB core material and Mg/Mg-20GMB hybrid composite have higher porosity than pure Mg. The presence of core Mg-20GMB in as-cast Mg/Mg-20GMB causes a reduction in experimental density when compared to as-cast pure magnesium, with a slight increase in the porosity value. Note that porosity and inclusions have a huge collapsing effect on the mechanical properties of metal matrix composites [28]. The porosity of as-cast composite is less than 2% (near net shape) and can be attributed to the presence of reinforcement and the entrapped gas during solidification [26,27]. The entrapment of gases predominantly relies upon the preparation strategy, for example, blending and pouring, holding time, and mixing speed. The position and size of the impeller can also have a significant effect on the porosity. Note that the density of the hybrid composite nicely comes between the density values of as-cast magnesium and core Mg-GMB core.

Table 1. Results of density and porosity measurements of monolithic and Mg/Mg-20GMB hybrid composite.

Materials	Theoretical Density (g/cc)	Experimental Density (g/cc)	Porosity (%)
as-cast pure Mg	1.738	1.712 ± 0.009	1.50
Mg-20GMB	1.537	1.492 ± 0.016	2.93
as-cast Mg/Mg-20GMB	1.680	1.651 ± 0.013	1.73

3.2. XRD Analysis

Figure 3 shows the X-ray diffraction (XRD) patterns of as-cast pure Mg and Mg/Mg-20GMB hybrid composite. The XRD pattern in Figure 3a for as-cast pure Mg shows only peaks corresponding to the α -Mg matrix, as expected. Mg-based hybrid composite peaks corresponding to Mg and Mg₂Si phases were observed in the case of as-cast Mg/Mg-20GMB hybrid composite (Figure 3b). Interfacial reactions between the Mg matrix and GMB particles in the Mg-20GMB core result in the formation of Mg₂Si

secondary phases. This conclusion is also supported by SEM observations and will be discussed in detail in the subsequent sections (Figures 4 and 5).

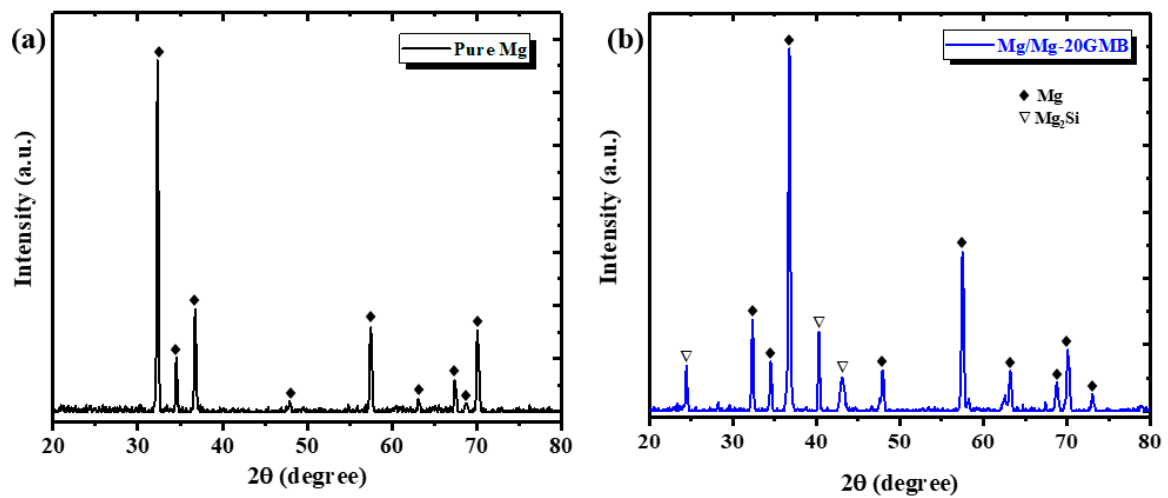


Figure 3. X-ray diffractograms of as-cast: (a) pure Mg and (b) Mg/Mg-20GMB hybrid composite.

3.3. Grain Size Analysis

Table 2 compares the grain sizes of the as-cast Mg/Mg-20GMB hybrid composite at the shell, interface, and core regions. The grain size at the shell, core, and interface regions were similar, considering the standard deviation. At the shell region, the grains are well-formed and equiaxed. At the interface region, the grains are generally smaller in size, and some are distorted and elongated in shape. At the core region, the grains are usually equiaxed in shape.

Table 2. The average grain size of as-cast Mg/Mg-20GMB hybrid composite.

Materials	Shell Region (μm)	Interface Region (μm)	Core Region (μm)
Mg/Mg-20GMB	35.44 ± 3.19	34.11 ± 2.30	33.65 ± 2.45

Grain refinement is critical for the strengthening of engineering alloys. Normally, the yield strength of a material is contrarily corresponding to the square root of grain size, as stated by the Hall-Petch equation:

$$\sigma = \sigma_0 + Kd^{-1/2} \quad (1)$$

where σ is the yield stress, σ_0 is the yield stress of a single crystal, K is a constant, and d is the grain size [29]. The value of K depends upon the number of slip systems and is larger for HCP metals as compared to face-centered cubic (FCC) and body-centered cubic (BCC) metals [30]. Therefore, HCP metals possess higher strength sensitivity to the grain size. In a metal matrix composite, the secondary reinforcing phase can have a remarkable impact on the grain size of the matrix. The grain refinement is caused by the various nucleations of the Mg phase on secondary particles, and that will restrict the development of the magnesium crystals due to the presence of rigid secondary phases.

3.4. Scanning Electron Microscopy (SEM) Analysis

Figure 4 shows the SEM micrographs of as-cast pure Mg and Mg/Mg-20GMB hybrid composite. From the figure, the surface of pure Mg is smooth and free of microstructural defects (Figure 4a). The interface between the Mg-shell and the Mg-20GMB core in the developed as-cast Mg/Mg-20GMB hybrid composite is shown in Figure 4b. It can be observed that the micrograph is composed of two distinct regions, while the shell region shows Mg, the core region is Mg-20GMB syntactic foam with white and grey phases. Further, the SEM micrograph also demonstrates a near clear interface

with metallurgical bonding between the shell and the core regions barring slight debonding at some interface locations, as observed in Figure 4b.

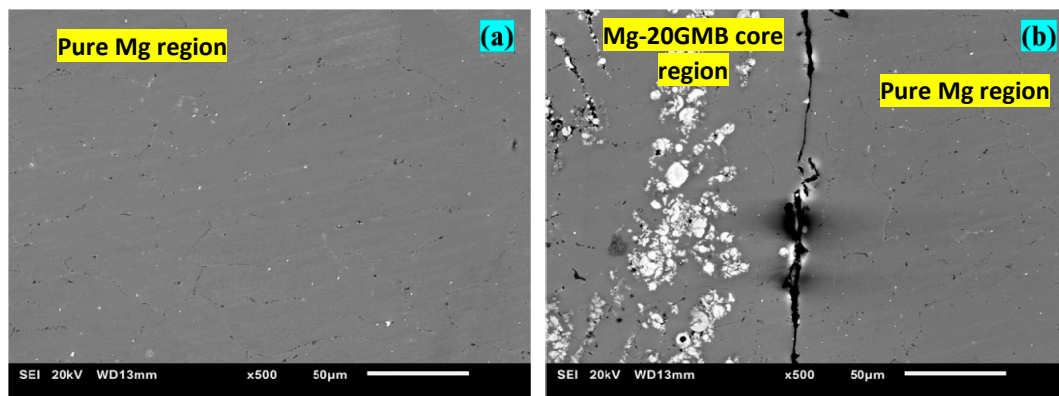


Figure 4. Scanning electron microscopy of as-cast: (a) pure Mg and (b) Mg/Mg-20GMB hybrid composite.

The lower homogenization temperature (250 °C) used in this study ensures greater stability of microspheres in the Mg-20GMB core and counteracts the healing of inter-particle porosity facilitated by the yielding of microspheres in higher melting temperature matrices. A further concern raised by the high reactivity of Mg is the possible formation of detrimental phases in the interface region between GMB particles and Mg matrix; this has been avoided by eliminating the sintering process for fabricating the core material, which resulted in minimal Mg₂Si secondary phase formation for Mg-20GMB core material. Constrained reaction areas are clearly noticeable along the walls of the glass spheres, which might prompt solid interfacial bonding between the matrix and GMB constituents. Minimally fractured GMB particles were observed due to carefully selected and optimized processing parameters. Higher magnification clearly shows the presence of Chinese script shaped Mg₂Si (Figure 5) in the Mg-GMB region. As Mg is highly reactive, a chemical reaction between Mg and SiO₂ is possible thermodynamically.

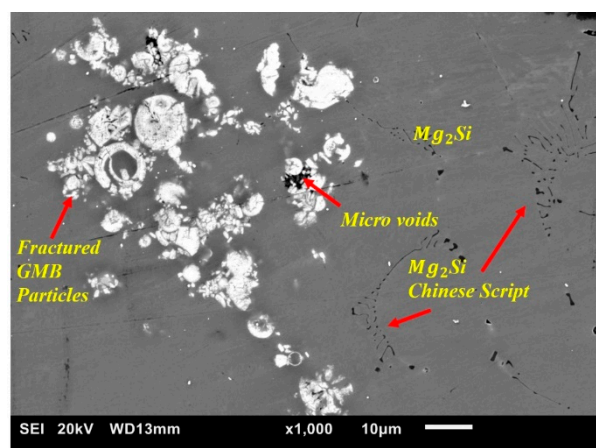


Figure 5. SEM image of Mg-20GMB core material under higher magnification.

3.5. Energy-Dispersive X-ray Spectroscopy (EDX)

Energy-dispersive X-ray spectroscopy analysis of as-cast pure Mg and Mg/Mg-20GMB hybrid composite was conducted to quantify the near-surface number of elements present in the composite;

the results are shown in Figure 6. The peaks obtained from the EDX results confirm the presence of magnesium and glass microballoon (SiO_2) elements in the Mg-based hybrid composite.

EDX analysis reveals the existence of Mg_2Si as a secondary phase in Mg-20GMB core syntactic foam. The diffusion of the Si atoms from the filled/fractured GMB particle shell into the Mg matrix may be the reason for the development of Mg_2Si (see the marked region in Figure 5). Silicon is nearly insoluble in magnesium with the solubility limit < 30 ppm (< 0.003 wt.%) [31]. A slight diffusion of Si atoms into Mg can result in precipitate formation, as observed in the current study as well. Therefore, the formation of a secondary phase like Mg_2Si cannot be restricted.

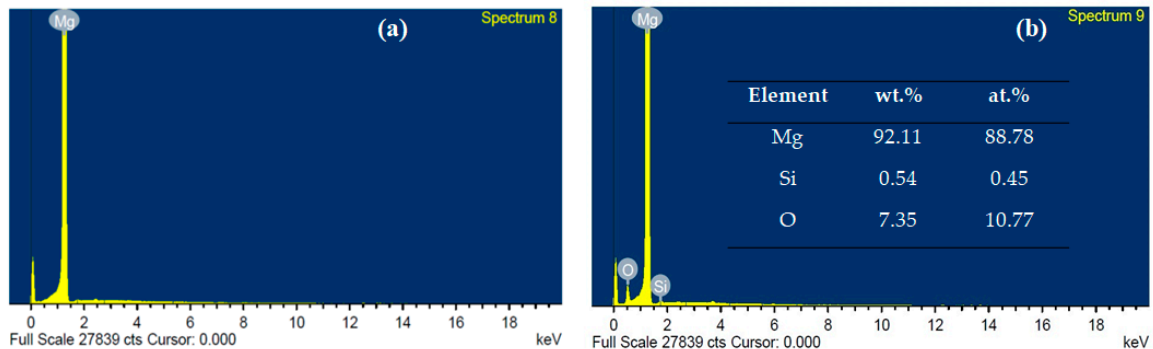


Figure 6. Energy dispersive X-ray spectroscopy (EDX) spectra of as-cast (a) pure Mg and (b) Mg/Mg-20GMB hybrid composite (the inset shows the element content).

3.6. Hardness

The results of hardness tests performed on the as-cast pure Mg shell, core, and the interface regions of the as-cast Mg/Mg-20GMB hybrid composite are listed in Table 3. The hardness of as-cast pure Mg is lower than the hardness of the as-cast Mg/Mg-20GMB hybrid composite. The Mg-20GMB core exhibits a significantly higher hardness value (80 ± 4 HV) compared to the Mg shell and the interface region. The relatively higher microhardness at the core and interface region can be attributed to strain localization, solid solution strengthening, and presence of harder GMB particles (5 Mohs scale compared to 2 Mohs scale of pure Mg) [20,32,33]. GMB particles restrain themselves from deformation in addition to constraining Mg's plastic deformation, resulting in such behavior.

Table 3. Microhardness values for as-cast Mg/Mg-20GMB hybrid composite.

Materials	Microhardness (Hv)		
	Shell Region	Core Region	Interface Region
as-cast pure Mg	44 ± 5	—	—
as-cast Mg/Mg-20GMB	53 ± 3	80 ± 4	74 ± 6

3.7. Compressive Behavior

The room temperature compression properties of the as-cast pure Mg and Mg/Mg-20GMB hybrid composite are shown in Figure 7, and corresponding data are summarized in Table 4. The obtained yield strength (YS) and ultimate compressive strength (UCS) of pure Mg are 88 ± 3 and 215 ± 5 MPa, respectively whereas the Mg/Mg-20GMB hybrid composite shows a YS and UCS of 151 ± 4 and 165 ± 3 MPa, respectively. The increment in YS of the Mg/Mg-20GMB hybrid composite was by $\uparrow 71.6\%$ and the drop in the UCS was by $\downarrow 23.25\%$ when compared to as-cast pure Mg.

It can also be observed from Table 4 that the yield strength of Mg/Mg-20GMB hybrid composite is superior or even comparable with other commercial cast Mg alloys. This can be attributed to the change in work hardening behavior and the competing load sharing between the shell and core material [33]. Further, it was interesting to note that the developed as-cast Mg/Mg-20GMB hybrid

composite exhibited a second work hardening phase after the failure of the Mg shell. For as-cast Mg/Mg-20GMB hybrid composite, the stress was transferred to the Mg-20GMB core when the Mg shell fractured. It was seen that the stress decreased after reaching a peak at the end of the linear elastic region and was followed by a plateau region. Thereafter, the load is experienced by the Mg-20GMB core. The compression behavior of the Mg-20GMB core is similar to the behaviors commonly observed for metal and polymer syntactic foams [20]. The plateau region appears at a constant stress level and slowly decreases. Incorporating porosity in the Mg-20GMB syntactic foam core through the addition of hollow GMB particles leads to a stress plateau at constant rate. Plastic deformation regime as observed in this study. The pores which are surrounded by stiff, strong GMB walls, impede the deformation and collapse during compressive loading; with further loadings deformed material occupies the porosity opened up due to fracture. Loading further makes progressive densification of the microstructure. Further, embedding porosity with the addition of 20 wt.% GMB in the core results in a decrease of the UCS value in the hybrid composite from 215 MPa to 165 MPa, as compared to as-cast pure Mg, due to reduction in load bearing area. The ductility of the hybrid composite is a combination of the ductility of the core and the shell. The ductility of the as-cast Mg/Mg-20GMB was ~186% higher than that of as-cast pure Mg.

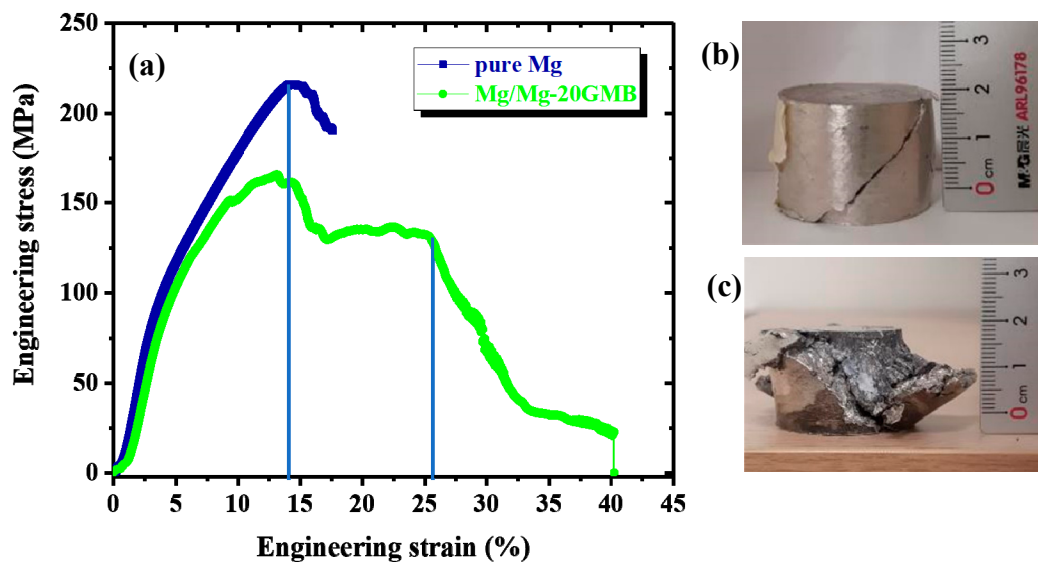


Figure 7. (a) Compression stress–strain graphs, and fracture appearance of (b) as-cast pure Mg, and (c) as-cast Mg/Mg-20GMB hybrid composite.

Table 4. Compression properties of as-cast pure Mg and Mg/Mg-20GMB hybrid composite and other reported commercial Mg alloys.

Materials	YS (MPa)	UCS (MPa)	Ductility (%)	Energy Absorption (MJ/m ³)
as-cast pure Mg	88 ± 3	215 ± 5	14.8 ± 0.3	36 ± 2.3
as-cast Mg/Mg-20GMB	151 ± 4 (↑71.6%)	165 ± 3 (↓23.25%)	42.4 ± 0.3 (↑186.48%)	51 ± 1.6 (↑41.66%)
AZ91E #	130	400	–	–
RZ5(ZE41) #	130–150	330–365	–	–
ZRE1(EZ33) #	85–120	275–340	–	–

denoted the data from the ASM metal alloy handbook. Note: YS = yield strength, UCS = ultimate compressive strength.

Mg/Mg-20GMB hybrid composite shows the maximum energy absorption (EA) value of 51 MJ/m³, which is ~41.66% greater than that of as-cast pure Mg. The core (Mg-20GMB) material resulted in a

stress plateau region, demonstrating constrained strain hardening during plastic deformation and resulting in improved energy absorption. The higher EA value for Mg/Mg-20GMB highlights functional interfacial integrity between the shell and core, thereby improving the deformability and hence making it suitable for intended use in load-bearing/crash scenarios.

3.8. Fractography Analysis

Figure 8 displays the typical fracture surfaces of as-cast pure Mg and Mg/Mg-20GMB hybrid composite after compressive loading. Figure 8a shows the SEM fractography of the as-cast pure Mg. It can be observed that the as-cast Mg exhibits rough fracture surfaces with the presence of shear bands. In the case of the Mg/Mg-20GMB hybrid composite, where particle crushing does not seem to be prominent, several intact GMB particles can be observed. Some broken particles (shown with an arrow) are also found on the failure surface shown in Figure 8b, but the number of such particles is small in this specimen. As shown in Figure 8b, several mechanisms can be identified, including matrix fracture and some GMBs pullout. The surface of the as-cast Mg/Mg-20GMB hybrid composite was much rougher than the surfaces of the as-cast pure magnesium specimens.

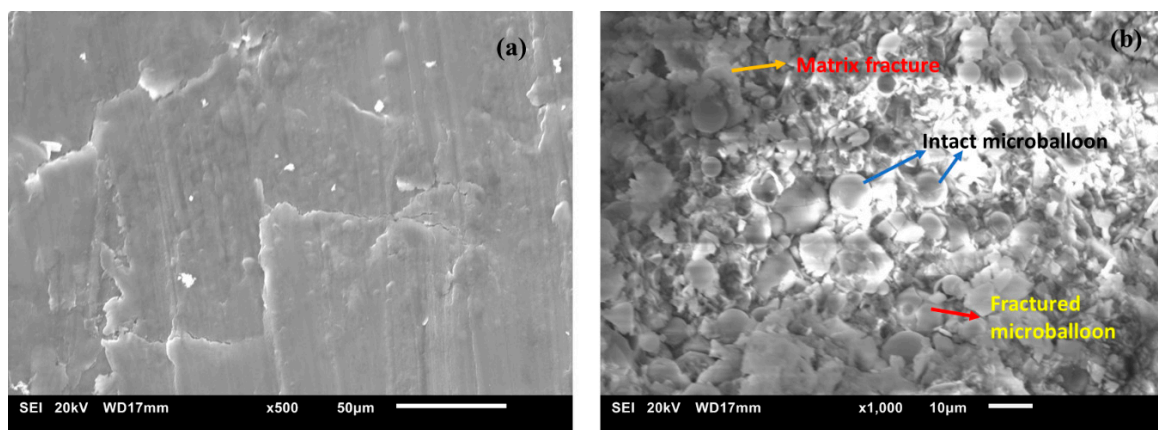


Figure 8. Fractography analysis of as-cast (a) pure Mg, and (b) Mg/Mg-20GMB hybrid composite.

4. Conclusions

As-cast pure Mg and Mg/Mg-20GMB hybrid composite were synthesized by using a combination of powder metallurgy (blending, compaction, and hot extrusion) and disintegrated melt deposition (DMD) techniques. The Mg/Mg-20GMB hybrid composite exhibited lower density and moderate metallurgical bonding between the Mg-shell and Mg-20GMB core regions. EDX results confirmed the presence of Mg₂Si as the secondary phase in the Mg-20GMB core material. The Mg-20GMB core showed higher hardness than the shell zone (pure Mg) due to the presence of a secondary phase (Mg₂Si) and the Mg/GMB interfacial regions. The increment of yield strength of the as-cast Mg/Mg-20GMB hybrid composite was by +71.6%, and a drop in the UCS by −23.3% was observed when compared to as-cast pure Mg. The shell-core structure provides a new way to improve the mechanical properties of the hybrid composites.

Author Contributions: M.G., B.W.C. and S.C.K.W.: conceptualization, methodology; J.G.Y.S. and P.R.M.: data curation, writing—original draft preparation; G.P. and V.M.: investigation; M.G.: supervision; P.R.M., G.P. and V.M.: writing—reviewing and editing. All authors have read and agreed to the published version of the manuscript.

Funding: This research was supported by the Agency for Science, Technology, and Research (A*STAR), Singapore, under its program “Manufacturing of lightweight free-form shell, sandwich, and hybrid cellular structures for aerospace component manufacturing and repair” (WBS # R 265 000 638 305).

Conflicts of Interest: The authors declare that there is no conflict of interest.

References

1. Gupta, M.; Parande, G.; Manakari, V. An insight into high performance magnesium alloy/nano-metastable-syntactic composites. In Proceedings of the 17th Australian International Aerospace Congress (AIAC 2017), Melbourne, VIC, Australia, 26–28 February 2017; Engineers Australia, Royal Aeronautical Society: Canberra, Australia, 2017; p. 270.
2. Hazeli, K.; Sadeghi, A.; Pekguleryuz, M.; Kotsos, A. Damping and dynamic recovery in magnesium alloys containing strontium. *Mater. Sci. Eng. A* **2014**, *589*, 275–279. [[CrossRef](#)]
3. Kujur, M.S.; Manakari, V.; Parande, G.; Tun, K.S.; Mallick, A.; Gupta, M. Enhancement of thermal, mechanical, ignition and damping response of magnesium using nano-ceria particles. *Ceram. Int.* **2018**, *44*, 15035–15043. [[CrossRef](#)]
4. Jensen, L.; Hansman, R.J.; Venuti, J.; Reynolds, T. Commercial airline altitude optimization strategies for reduced cruise fuel consumption. In Proceedings of the 14th AIAA Aviation Technology, Integration, and Operations Conference, Atlanta, GA, USA, 16–20 June 2014; p. 3006.
5. Manakari, V.; Parande, G.; Gupta, M. Selective laser melting of magnesium and magnesium alloy powders: A review. *Metals* **2017**, *7*, 2. [[CrossRef](#)]
6. Shulin, X.; Gupta, M. Using lanthanum to enhance the overall ignition, hardness, tensile and compressive strengths of mg-0.5 zr alloy. *J. Rare Earths* **2017**, *35*, 723.
7. Matli, P.R.; Krishnan, A.V.; Manakari, V.; Parande, G.; Chua, B.; Wong, S.; Lim, C.; Gupta, M. A new method to lightweight and improve strength to weight ratio of magnesium by creating a controlled defect. *J. Mater. Res. Technol.* **2020**, *9*, 3664–3675. [[CrossRef](#)]
8. Parande, G.; Manakari, V.; Meenashisundaram, G.K.; Gupta, M. Enhancing the tensile and ignition response of monolithic magnesium by reinforcing with silica nanoparticulates. *J. Mater. Res.* **2017**, *32*, 2169–2178. [[CrossRef](#)]
9. Clyne, T.; Withers, P. *An Introduction to Metal Matrix Composites*; Cambridge University Press: Cambridge, UK, 1995.
10. Paramsothy, M.; Gupta, M.; Srikanth, N. Processing, microstructure, and properties of a mg/al bimetal macrocomposite. *J. Compos. Mater.* **2008**, *42*, 2567–2584. [[CrossRef](#)]
11. Reddy, M.P.; Manakari, V.; Parande, G.; Ubaid, F.; Shakoor, R.; Mohamed, A.; Gupta, M. Enhancing compressive, tensile, thermal and damping response of pure al using bn nanoparticles. *J. Alloys Compd.* **2018**, *762*, 398–408. [[CrossRef](#)]
12. Parande, G.; Manakari, V.; Koppaarthi, S.D.S.; Gupta, M. A study on the effect of low-cost eggshell reinforcement on the immersion, damping and mechanical properties of magnesium–zinc alloy. *Compos. Part B Eng.* **2020**, *182*, 107650. [[CrossRef](#)]
13. Ferkel, H.; Mordike, B. Magnesium strengthened by sic nanoparticles. *Mater. Sci. Eng. A* **2001**, *298*, 193–199. [[CrossRef](#)]
14. Hassan, S.; Tan, M.; Gupta, M. Development of nano-zro2 reinforced magnesium nanocomposites with significantly improved ductility. *Mater. Sci. Technol.* **2007**, *23*, 1309–1312. [[CrossRef](#)]
15. Michels, W. Magnesium alloys and their applications. *Mater. Technol.* **1998**, *13*, 121–122. [[CrossRef](#)]
16. Mordike, B.; Ebert, T. Magnesium: Properties—Applications—Potential. *Mater. Sci. Eng. A* **2001**, *302*, 37–45. [[CrossRef](#)]
17. Marker, T. *Evaluating the Flammability of Various Magnesium Alloys during Laboratory- and Full-Scale Aircraft Fire Test*; DOT/FAA/AR-11/3; US Department of Transportation, Federal Aviation Administration: Atlantic City, NJ, USA, 2013.
18. Papis, K.J.; Loeffler, J.F.; Uggowitzer, P.J. Light metal compound casting. *Sci. China Ser. E Technol. Sci.* **2009**, *52*, 46–51. [[CrossRef](#)]
19. Yung, K.; Zhu, B.; Yue, T.; Xie, C. Preparation and properties of hollow glass microsphere-filled epoxy-matrix composites. *Compos. Sci. Technol.* **2009**, *69*, 260–264. [[CrossRef](#)]
20. Manakari, V.; Parande, G.; Doddamani, M.; Gupta, M. Enhancing the ignition, hardness and compressive response of magnesium by reinforcing with hollow glass microballoons. *Materials* **2017**, *10*, 997. [[CrossRef](#)] [[PubMed](#)]
21. Manakari, V.; Parande, G.; Gupta, M. Effects of hollow fly-ash particles on the properties of magnesium matrix syntactic foams: A review. *Mater. Perform. Charact.* **2016**, *5*, 116–131. [[CrossRef](#)]

22. Doddamani, M. Wear behavior of glass microballoon based closed cell foam. *Mater. Res. Express* **2019**, *6*, 115314. [[CrossRef](#)]
23. Manakari, V.; Parande, G.; Doddamani, M.; Gupta, M. Evaluation of wear resistance of magnesium/glass microballoon syntactic foams for engineering/biomedical applications. *Ceram. Int.* **2019**, *45*, 9302–9305. [[CrossRef](#)]
24. Hu, Y.; Chen, Y.-Q.; Li, L.; Hu, H.-D.; Zhu, Z.-A. Microstructure and properties of al/cu bimetal in liquid–Solid compound casting process. *Trans. Nonferrous Metal. Soc.* **2016**, *26*, 1555–1563. [[CrossRef](#)]
25. Liu, J.; Hu, J.; Nie, X.; Li, H.; Du, Q.; Zhang, J.; Zhuang, L. The interface bonding mechanism and related mechanical properties of mg/al compound materials fabricated by insert molding. *Mater. Sci. Eng. A* **2015**, *635*, 70–76. [[CrossRef](#)]
26. Brandes, E.A.; Brook, G. *Smithells Metals Reference Book*; Elsevier: Amsterdam, The Netherlands, 2013.
27. Parande, G.; Manakari, V.; Wakeel, S.; Kujur, M.S.; Gupta, M. Enhancing mechanical response of monolithic magnesium using nano-niti (nitinol) particles. *Metals* **2018**, *8*, 1014. [[CrossRef](#)]
28. Kujur, M.S.; Mallick, A.; Manakari, V.; Parande, G.; Tun, K.S.; Gupta, M. Significantly enhancing the ignition/compression/damping response of monolithic magnesium by addition of Sm₂O₃ nanoparticles. *Metals* **2017**, *7*, 357. [[CrossRef](#)]
29. Reddy, M.P.; Ubaid, F.; Shakoor, R.; Parande, G.; Manakari, V.; Mohamed, A.; Gupta, M. Effect of reinforcement concentration on the properties of hot extruded Al–Al₂O₃ composites synthesized through microwave sintering process. *Mater. Sci. Eng. A* **2017**, *696*, 60–69. [[CrossRef](#)]
30. Parande, G.; Manakari, V.; Koppaarthi, S.D.S.; Gupta, M. Utilizing low-cost eggshell particles to enhance the mechanical response of mg–2.5 zn magnesium alloy matrix. *Adv. Eng. Mater.* **2018**, *20*, 1700919. [[CrossRef](#)]
31. Mayencourt, C.; Schaller, R. Development of a high-damping composite: Mg₂Si/Mg. *Phys. Status Solidi A* **1997**, *163*, 357–368. [[CrossRef](#)]
32. Krishna, B.V.; Venugopal, P.; Rao, K.P. Solid state joining of dissimilar sintered p/m preform tubes by simultaneous cold extrusion. *Mater. Sci. Eng. A* **2004**, *386*, 301–317. [[CrossRef](#)]
33. Paramsothy, M.; Srikanth, N.; Gupta, M. Solidification processed mg/al bimetal macrocomposite: Microstructure and mechanical properties. *J. Alloys Compd.* **2008**, *461*, 200–208. [[CrossRef](#)]



© 2020 by the authors. Licensee MDPI, Basel, Switzerland. This article is an open access article distributed under the terms and conditions of the Creative Commons Attribution (CC BY) license (<http://creativecommons.org/licenses/by/4.0/>).